

A multigrid solver for PDE-constrained optimization with uncertain inputs

Gabriele Ciaramella¹, Fabio Nobile² and Tommaso Vanzan^{2*}

¹MOX, Dipartimento di Matematica, Politecnico di Milano, Italy.

^{2*}CSQI Chair, Institute of Mathematics, Ecole Polytechnique Fédérale de Lausanne, Switzerland.

*Corresponding author(s). E-mail(s): tommaso.vanzan@epfl.ch;

Contributing authors: gabriele.ciaramella@polimi.it;

fabio.nobile@epfl.ch;

Abstract

We present a multigrid algorithm to solve efficiently the large saddle-point systems of equations that typically arise in PDE-constrained optimization under uncertainty. The algorithm is based on a collective smoother that at each iteration sweeps over the nodes of the computational mesh, and solves a reduced saddle-point system whose size depends on the number N of samples used to discretized the probability space. We show that this reduced system can be solved with optimal $\mathcal{O}(N)$ complexity. We test the multigrid method both as a stationary method and as a preconditioner for GMRES on three problems: a linear-quadratic problem for which the multigrid method is used to solve directly the linear optimality system; a nonsmooth problem with box constraints and L^1 -norm penalization on the control, in which the multigrid scheme is used as an inner solver within a semismooth Newton iteration; a risk-adverse problem with the smoothed CVaR risk measure where the multigrid method is called within a preconditioned Newton iteration. In all cases, the multigrid algorithm exhibits excellent performances and robustness with respect to all parameters of interest.

Keywords: multigrid, optimization under uncertainty, random PDEs

MSC Classification: 65M55 - 65F10 - 65K10 - 49J55

with A_j and A_j^\top for $j = 1, \dots, N$ [10]. For a full-space formulation, block diagonal preconditioners have been proposed in [11] and studied in [12], using both an algebraic approach based on Schur complement approximations, and an operator preconditioning framework.

In this manuscript, we present a multigrid method to solve general problems of the form (1) and show how this strategy can be used for the efficient solution of three different Optimal Control Problems Under Uncertainty (OCPUU). First, we consider a linear-quadratic OCPUU and use the multigrid algorithm directly to solve the linear optimality system. Second, we consider a nonsmooth OCPUU with box constraints and L^1 regularization on the control. To solve such problem, we use the collective multigrid method as an inner solver within an outer semismooth Newton iteration. Incidentally, we show that the theory developed for the deterministic OCPs with L^1 regularization can be naturally extended to the class of OCPUU considered here. Third, we study a risk-averse OCPUU involving the smoothed Conditional Value at Risk (CVaR) and test the performance of the multigrid scheme in the context of a nonlinear preconditioned Newton method.

The multigrid algorithm is based on a collective smoother [13–15] that, at each iteration, loops over all nodes of the computational mesh (possibly in parallel), collects all the degrees of freedom related to a node, and updates them collectively by solving a reduced saddle-point problem. For classical (deterministic) PDE-constrained optimization problems, this reduced system has size 3×3 so that its solution is immediate [14]. In our context, the reduced problem has size $(2N + 1) \times (2N + 1)$, so that it can be large when dealing with a large number of samples. Fortunately, we show that it can be solved with optimal $O(N)$ complexity. Let us remark that collective multigrid strategies have been applied to OCPUU in [16, 17] and in [18]. This manuscript differs from the mentioned works since, on the one hand, [16, 17] considers a *stochastic* control u , therefore for (almost) every realization of the random parameters a different control $u(\omega)$ is computed through the solution of a standard deterministic OCP. On the other hand, [18] considers a Stochastic Galerkin discretization, and hence the corresponding optimality system has a structure which is very different from (2).

The multigrid algorithm presented here assumes that all variables are discretized on the same finite element mesh. Further, despite we here consider only the case of a global distributed control, the smoothing procedure could be extended to a local distributed control on a subset $\tilde{\mathcal{D}}$ of the computational domain \mathcal{D} , and to boundary control, see, e.g., [13].

Finally, we remark that the multigrid solver proposed is based on a hierarchy of spatial discretizations corresponding to different levels of approximation, but the discretization of the probability space remains fixed, that is, the number of samples remains constant across the multigrid hierarchy. The extension of the multigrid algorithm to coarsening procedures also in the probability

space will be the subject of future endeavours. Nevertheless, the multigrid algorithm can already be incorporated within outer optimization routines that use different levels of approximations of the probability space, see, e.g., [7, 10, 19].

The rest of the manuscript is organized as follows. In Section 2 we introduce the notation, a classical linear-quadratic OCPUU, and interpret (2) as the matrix associated to an optimality system of the discretized OCPUU. In Section 3, we present the collective multigrid algorithm, discuss implementation details and show its performance to solve the linear-quadratic OCPUU. In Section 4, we consider a nonsmooth OCPUU with box constraints and a L^1 regularization on the control. Section 5 deals with a risk-adverse OCPUU. For each of these cases, we first show how the multigrid approach can be integrated into the solution process, by detailing concrete algorithms, and then we present extensive numerical experiments to show the efficiency of the proposed framework. Finally, we draw our conclusions in Section 6.

2 A linear-quadratic optimal control problem under uncertainty

Let $\mathcal{D} \subset \mathbb{R}^d$ be a Lipschitz bounded domain, V the standard Sobolev space $H_0^1(D)$, and $(\Omega, \mathcal{F}, \mathbb{P})$ a complete probability space. Given a function $u \in L^2(\mathcal{D})$, we consider the linear elliptic random PDE

$$a_\omega(y, v) = (u, v), \forall v \in V, \quad \mathbb{P}\text{-a.e. } \omega \in \Omega, \quad (4)$$

where $a_\omega(\cdot, \cdot) : V \times V \rightarrow \mathbb{R}$ is a bilinear form and (\cdot, \cdot) denotes the standard $L^2(\mathcal{D})$ scalar product. To assure uniqueness and sufficient integrability of the solution of (4), we make the following additional assumption.

Assumption 1 *There exist two random variables $a_{\min}(\omega)$ and $a_{\max}(\omega)$ such that*

$$0 < a_{\min}(\omega) \|v\|_V^2 \leq a_\omega(v, v) \leq a_{\max}(\omega) \|v\|_V^2, \quad \forall v \in V, \quad \mathbb{P}\text{-a.e. } \omega \in \Omega,$$

and further a_{\min}^{-1} and a_{\max} are in $L^p(\Omega)$ for some $p \geq 4$.

Under Assumption 1, it is well-known (see, e.g., [20, 21]) that (4) admits a solution in V for \mathbb{P} -a.e. ω , and the solution y , interpreted as a function-valued random variable $y : \omega \in \Omega \mapsto y(\omega) \in V$, lies in the Bochner space $L^q(\Omega; V)$, $q \leq p$, [22]. We often use the shorthand notation $y_\omega = y(\cdot, \omega)$ when the dependence on x is not needed, or $y_\omega(u)$ when we want to highlight the dependence on the control function u .

In this manuscript, we consider the minimization of functionals constrained by (4). Let us first focus on the linear-quadratic problem

$$\begin{aligned} & \min_{u \in L^2(\mathcal{D}), y \in L^2(\Omega; V)} \frac{1}{2} \mathbb{E} \left[\|y_\omega - y_d\|_{L^2(\mathcal{D})}^2 \right] + \frac{\nu}{2} \|u\|_{L^2(\mathcal{D})}^2, \\ & \text{subject to} \\ & a_\omega(y_\omega, v) = (u + f, v), \quad \forall v \in V, \mathbb{P}\text{-a.e. } \omega \in \Omega, \end{aligned} \quad (5)$$

where $y_d \in L^2(\mathcal{D})$ is a target state, $f \in L^2(\mathcal{D})$, $\mathbb{E} : L^1(\Omega) \rightarrow \mathbb{R}$ is the expectation operator and $\nu > 0$.¹ Introducing the linear control-to-state map $S : u \in L^2(\mathcal{D}) \rightarrow y_\omega(u) \in L^2(\Omega; L^2(\mathcal{D}))$, we reformulate (5) as,

$$\min_{u \in L^2(\mathcal{D})} \frac{1}{2} \mathbb{E} \left[\|S(u) - y_d\|_{L^2(\mathcal{D})}^2 \right] + \frac{\nu}{2} \|u\|_{L^2(\mathcal{D})}^2. \quad (6)$$

Existence and uniqueness of the minimizer of (6) follows directly from standard variational arguments [1, 23–25]. Furthermore, due to Assumption 1, the optimal control \bar{u} satisfies the variational equality

$$(\nu \bar{u} - S^*(y_d - S(\bar{u} + f)), v)_{L^2(\mathcal{D})} = 0, \quad \forall v \in L^2(\mathcal{D}), \quad (7)$$

where the adjoint operator $S^* : L^2(\Omega; L^2(\mathcal{D})) \rightarrow L^2(\mathcal{D})$, satisfying $(Su, z)_{L^2(\Omega; L^2(\mathcal{D}))} = (u, S^*z)_{L^2(\mathcal{D})}$, is characterized by $S^*z = \mathbb{E}[p]$ where $p = p_\omega(x)$ is the solution of the adjoint equation

$$a_\omega(v, p_\omega) = (z(\omega), v), \quad \forall v \in V, \mathbb{P}\text{-a.e. } \omega \in \Omega. \quad (8)$$

The optimality condition (7) can thus be formulated as the optimality system

$$\begin{aligned} & a_\omega(y_\omega, v) = (\bar{u} + f, v), \quad \forall v \in V, \mathbb{P}\text{-a.e. } \omega \in \Omega, \\ & a_\omega(v, p_\omega) = (y_d - y_\omega, v), \quad \forall v \in V, \mathbb{P}\text{-a.e. } \omega \in \Omega, \\ & (\nu \bar{u} - \mathbb{E}[p_\omega], v)_{L^2(\mathcal{D})} = 0, \quad \forall v \in L^2(\mathcal{D}). \end{aligned} \quad (9)$$

To solve numerically (5), we replace the exact expectation operator \mathbb{E} of the objective functional by a quadrature formula $\widehat{\mathbb{E}}$ with N nodes $\{\omega_i\}_{i=1}^N$ and positive weights $\{\zeta_i\}_{i=1}^N$, namely

$$\mathbb{E}[X] \approx \widehat{\mathbb{E}}[X] := \sum_{i=1}^N \zeta_i X(\omega_i), \quad \text{with} \quad \sum_{i=1}^N \zeta_i = 1.$$

Common quadrature formulae are Monte Carlo, Quasi-Monte Carlo and Gaussian formulae. The latter requires that the probability space can be

¹To keep a light notation here and in the following sections, we omitted the continuous embedding operators from $L^2(\Omega; V)$ to $L^2(\Omega; L^2(\mathcal{D}))$ and from $L^2(\mathcal{D})$ to V' , see, e.g., [23, Section 2.13].

which collect the degrees of freedom associated to the i -th node, the scalar $u_i = (\mathbf{u})_i$, and the restriction operators $R_i \in \mathbb{R}^{(2N+1)N_h \times 2N+1}$ such that

$$R_i \begin{pmatrix} \mathbf{y} \\ \mathbf{u} \\ \mathbf{p} \end{pmatrix} = \begin{pmatrix} \tilde{\mathbf{y}}_i \\ u_i \\ \tilde{\mathbf{p}}_i \end{pmatrix} =: \mathbf{x}_i.$$

The prolongation operators are $P_i := R_i^\top$, while the reduced matrices $\tilde{S}_i := R_i S P_i \in \mathbb{R}^{2N+1 \times 2N+1}$ represent a condensed saddle-point matrix on the i -th node, and satisfy

$$\tilde{S}_i = \begin{pmatrix} \text{diag}(\mathbf{c}_i) & 0 & \text{diag}(\mathbf{a}_i) \\ 0 & (G)_{i,i} & \mathbf{d}_i^\top \\ \text{diag}(\mathbf{a}_i) & \mathbf{e}_i & 0 \end{pmatrix} \quad (11)$$

with $\mathbf{c}_i := ((C_1)_{i,i}, \dots, (C_N)_{i,i})^\top$, $\mathbf{a}_i := ((A_1)_{i,i}, \dots, (A_N)_{i,i})^\top$, $\mathbf{e}_i := ((E_1)_{i,i}, \dots, (E_N)_{i,i})^\top$, $\mathbf{d}_i = ((D_1)_{i,i}, \dots, (D_N)_{i,i})^\top$, where $\text{diag}(\mathbf{v})$ denotes a diagonal matrix with the components of \mathbf{v} on the main diagonal.

Given an initial vector \mathbf{x}^0 , a Jacobi-type collective smoothing iteration computes for $n = 1, \dots, n_1$,

$$\mathbf{x}^n = (1 - \theta)\mathbf{x}^{n-1} + \theta \sum_{i=1}^{N_h} P_i \tilde{S}_i^{-1} R_i (\mathbf{f} - S\mathbf{x}^{n-1}), \quad (12)$$

where $\theta \in (0, 1]$ is a damping parameter. Gauss-Seidel variants can straightforwardly be defined. Next, we consider a sequence of meshes $\{\mathcal{T}_{h_\ell}\}_{\ell=\ell_{\min}}^{\ell_{\max}}$, which we assume for simplicity to be nested, and restriction and prolongator operators $R_{\ell-1}^\ell$, $P_{\ell-1}^\ell$ which map between grids $\mathcal{T}_{h_{\ell-1}}$ and \mathcal{T}_{h_ℓ} . In the numerical experiments, the coarse matrices are defined recursively in a Galerkin fashion starting from the finest one, namely $S_\ell := R_\ell^{\ell+1} S_{\ell+1} P_\ell^{\ell+1}$ for $\ell \in \{1, \dots, \ell_{\max} - 1\}$. Nevertheless it is obviously possible to define S_ℓ as the discretization of the continuous saddle-point system onto the mesh \mathcal{T}_{h_ℓ} . With this notation, the V-cycle collective multigrid is described by Algorithm 1, which can be repeated until a certain stopping criterium is satisfied. We used the notation *Collective_Smoothing*(\cdot, \cdot, \cdot) to denote possible variants of (12) (e.g. Gauss-Seidel).

Notice that (12) requires to invert the matrices S_i for each computational node. We now show that this can be done with optimal $O(N)$ complexity. Indeed, performing a Schur complement on u_i , the system $\tilde{S}_i \mathbf{x}_i = \mathbf{f}_i$, with $\mathbf{f}_i = (\mathbf{f}_{p_i}, b_{u_i}, \mathbf{f}_{y_i})^\top$ can be solved exclusively computing inverses of diagonal matrices and scalar products between vectors through

$$\begin{aligned} u_i &= \frac{b_{u_i} + \mathbf{d}_i^\top (\text{diag}(\mathbf{a}_i)^{-1} \text{diag}(\mathbf{c}_i) \text{diag}(\mathbf{a}_i)^{-1} \mathbf{f}_{y_i} - \text{diag}(\mathbf{a}_i)^{-1} \mathbf{f}_{p_i})}{(G)_{i,i} + \mathbf{d}_i^\top \text{diag}(\mathbf{a}_i)^{-1} \text{diag}(\mathbf{c}_i) \text{diag}(\mathbf{a}_i)^{-1} \mathbf{e}_i}, \\ \tilde{\mathbf{y}}_i &= (\text{diag}(\mathbf{a}_i))^{-1} (\mathbf{f}_{y_i} - \mathbf{e}_i u_i), \\ \tilde{\mathbf{p}}_i &= (\text{diag}(\mathbf{a}_i))^{-1} (\mathbf{f}_{p_i} - \text{diag}(\mathbf{c}_i) \tilde{\mathbf{y}}_i). \end{aligned} \quad (13)$$

Algorithm 1 V-cycle Collective Multigrid Algorithm - V-cycle($\mathbf{x}^0, \mathbf{f}, \ell$)

```

1: if  $\ell = \ell_{\min}$ , then
2:   set  $\mathbf{x}^0 = S_{\ell_{\min}}^{-1} \mathbf{f}$ . (direct solver)
3: else
4:    $\mathbf{x}^{n_1} = \text{Collective\_Smoothing}(\mathbf{x}^0, S_\ell, n_1)$  ( $n_1$  steps of coll. smoothing)
5:    $\mathbf{r} = \mathbf{f} - S_\ell \mathbf{x}^{n_1}$  (compute the residual)
6:    $\mathbf{e}_c = \text{V-cycle}(\mathbf{0}, R_{\ell-1}^\ell \mathbf{r}, \ell - 1)$ . (recursive call)
7:    $\mathbf{x}^0 = \mathbf{x}^{n_1} + P_{\ell-1}^\ell \mathbf{e}_c$  (coarse correction)
8:    $\mathbf{x}^{n_2} = \text{Collective\_Smoothing}(\mathbf{x}^0, S_\ell, n_2)$  ( $n_2$  steps of coll. smoothing)
9:   Set  $\mathbf{x}^0 = \mathbf{x}^{n_2}$  (update)
10: end if
11: return  $\mathbf{x}^0$ .

```

Notice that we should guarantee that $\text{diag}(\mathbf{a}_i)$ admits an inverse and that $(G)_{i,i} + \mathbf{d}_i^\top \text{diag}(\mathbf{a}_i)^{-1} \text{diag}(\mathbf{c}_i) \text{diag}(\mathbf{a}_i)^{-1} \mathbf{e}_i \neq 0$. This has to be verified case by case, so we now focus on the specific matrix (10). On the one hand, the vectors \mathbf{a}_i are strictly positive componentwise, since $(\mathbf{a}_i)_j = a_{\omega_j}(\phi_i, \phi_i) > 0 \forall i = 1, \dots, N_h, j = 1, \dots, N$ (due to Assumption 1). On the other hand, $(G)_{i,i} = \int_{\mathcal{D}} \phi_i^2(x) dx > 0$, while a direct calculation shows that

$$\mathbf{d}_i^\top \text{diag}(\mathbf{a}_i)^{-1} \text{diag}(\mathbf{c}_i) \text{diag}(\mathbf{a}_i)^{-1} \mathbf{e}_i = (M_s)_{i,i}^3 \sum_{j=1}^N w_j (A_j)_{i,i}^{-2} > 0,$$

which implies that (13) is well-defined.

Assuming that the V-cycle algorithm requires a constant number of iterations to reach a given tolerance as both N_h , N and the number of levels increase (so that the size of the coarse problem becomes negligible in the limit), Algorithm 1 exhibits an overall optimal linear complexity $O(N_h N)$ since asymptotically the cost of each iteration is dominated by the N_h relaxation steps, each of a cost proportional to N due to the above discussion. In the next numerical experiments sections, we show indeed that the number of iterations remain constant for several test cases.

3.1 Numerical experiments

We now show the performance of Alg. 1 and its robustness with respect to several parameters for the solution of (10). We consider the state equation

$$a_\omega(y_\omega, v) = \int_{\mathcal{D}} \kappa(x, \omega) \nabla y(x, \omega) \cdot \nabla v(x) dx = \int_{\mathcal{D}} u(x) v(x) dx, \quad \forall v \in V, \mathbb{P}\text{-a.e. } \omega \in \Omega, \quad (14)$$

in a domain $\mathcal{D} = (0, 1)^2$ discretized with a regular mesh of squares of edge $h_\ell = 2^{-\ell}$, which are then decomposed into two right triangles. We choose

$\kappa(x, \omega)$ as an approximated log-normal diffusion field

$$\kappa(x, \omega) = e^{\sigma \sum_{j=1}^M \sqrt{\lambda_j} b_j(x) N_j(\omega)} \approx e^{g(x, \omega)}, \quad (15)$$

where $g(x, \omega)$ is a mean zero Gaussian field with Covariance function $Cov_g(x, y) = \sigma^2 e^{-\frac{\|x-y\|_2^2}{L^2}}$. The parameter σ^2 tunes the variance of the random field, while L denotes the correlation length. The pairs $(b_j(x), \sigma^2 \lambda_j)$ are the eigenpairs of $T : L^2(\mathcal{D}) \rightarrow L^2(\mathcal{D})$, $(Tf)(x) = \int_{\mathcal{D}} Cov_g(x, y) f(y) dy$, and $N_j \sim \mathcal{N}(0, 1)$. Assumption 1 is satisfied since $a_{\min}(\omega) = (\text{ess inf}_{x \in \mathcal{D}} \kappa(x, \omega))^{-1}$ and $a_{\max}(\omega) = \|\kappa(\cdot, \omega)\|_{L^\infty(\mathcal{D})}$ are in $L^p(\Omega)$ for every $p < \infty$ [26]. We first consider $L^2 = 0.5$, so that setting $M = 3$ into (15) is enough to keep 99% of the variance, and we discretize the problem using the Stochastic Collocation method [27] on Gauss-Hermite tensorized quadrature nodes. The target state is $y_d = e^{y^2} \sin(2\pi x) \sin(2\pi y)$.

Table 1 shows the number of V-cycle iterations (Alg. 1) and of GMRES iterations preconditioned by the V-cycle in brackets to solve (10) up to a tolerance of 10^{-9} on the relative (unpreconditioned) residual. Inside the V-cycle algorithm, we use $n_1 = n_2 = 2$ pre- and post-smoothing iterations based on the Jacobi relaxation (12) with a damping parameter $\theta = 0.5$. The number of levels of the V-cycle hierarchy is denoted with N_L .

Table 1 Number of V-cycle iterations and preconditioned GMRES iterations (in brackets) to solve (10).

| | | | | |
|---|-----------|-----------|-----------|-----------|
| ν | 10^{-2} | 10^{-4} | 10^{-6} | 10^{-8} |
| It. | 17 (11) | 19 (13) | 19 (15) | 19 (14) |
| $N_h = 961, N = 125, N_L = 3, \sigma^2 = 0.5, L^2 = 0.5.$ | | | | |
| σ^2 | 0.1 | 0.5 | 1 | 1.5 |
| It. | 19 (12) | 19 (13) | 19 (13) | 19 (14) |
| $N_h = 961, N = 125, N_L = 3, \nu = 10^{-4}, L^2 = 0.5.$ | | | | |
| $N_h(N_L)$ | 225 (2) | 961 (3) | 3969 (4) | |
| It. | 18 (13) | 19 (13) | 19 (13) | |
| $N = 125, \nu = 10^{-4}, \sigma^2 = 0.5, L^2 = 0.5.$ | | | | |
| N | 8 | 27 | 64 | 125 |
| It. | 19 (12) | 19 (12) | 19 (13) | 19 (13) |
| $N_h = 961, \nu = 10^{-4}, \sigma^2 = 0.5, L^2 = 0.5.$ | | | | |

The multigrid algorithm has a perfect robustness with respect to all parameters considered. In particular, the convergence does not deteriorate as $\nu \rightarrow 0$, which is a well-known troublesome limit for several preconditioners (see, e.g., [12, 28–30] and references therein). Further, the third sub-table shows the robustness of the algorithm with respect to the number of levels as the fine grid is refined. The fourth sub-table instead shows that the number of iteration remains constant as the discretization of the probability space is refined.

Table 2 Number of V-cycle iterations and preconditioned GMRES iterations (in brackets) to solve (10).

| | | |
|-----|---------|---------|
| N | 100 | 1000 |
| It. | 21 (14) | 21 (14) |

$N_h = 3969$, $\nu = 10^{-4}$, $N_L = 3$, $\sigma^2 = 1.5$, $L^2 = 0.025$.

As a complementary experiment, we next consider $L^2 = 0.025$ and use the Monte Carlo method, since Stochastic Collocation suffers from the curse of dimensionality. We also refine the spatial grid to properly capture the variations of the random diffusion coefficient. Table 2 confirms the robustness of the algorithm even for much larger numbers of samples.

4 An optimal control problem under uncertainty with box-constraints and L^1 penalization

In this section, we consider the nonsmooth OCPUU

$$\begin{aligned} \min_{u \in U_{ad}} \frac{1}{2} \mathbb{E} \left[\|y_\omega(u) - y_d\|_{L^2(\mathcal{D})}^2 \right] + \frac{\nu}{2} \|u\|_{L^2(\mathcal{D})}^2 + \beta \|u\|_{L^1(\mathcal{D})}, \\ \text{subject to} \\ a_\omega(y_\omega(u), v) = (u + f, v), \quad \forall v \in V, \quad \mathbb{P}\text{-a-e. } \omega \in \Omega, \\ U_{ad} := \{v \in L^2(\mathcal{D}) : a \leq u \leq b \text{ almost everywhere in } \mathcal{D}\}, \end{aligned} \quad (16)$$

with $a < 0 < b$ and $\nu, \beta > 0$. Deterministic OCPs with a L^1 penalization lead to optimal controls which are sparse, i.e. they are nonzero only on certain regions of the domain \mathcal{D} [31, 32]. Sparse controls can be of great interest in applications, because it is often not desirable, or even impossible, to control the system over the whole domain \mathcal{D} . For sparse OCPUU, we mention [33] where the authors considered both a simplified version of (16) in which the randomness enters linearly into the state equation as a force term, and a different optimization problem whose goal is to find a stochastic control $u(\omega)$ which has a similar sparsity pattern regardless of the realization ω . Notice further that the assumption $\nu > 0$ does not eliminate the nonsmoothness of the objective functional, but it regularizes the optimal solution u , and is needed to use the fast optimization algorithm described in the following.

The well-posedness of (16) follows directly from standard variational arguments [23, 25], being U_{ad} a convex set, $\varphi(u) := \beta \|u\|_{L^1(\mathcal{D})}$ a convex function and the objective functional coercive. In particular, the optimal solution \bar{u} satisfies the variational inequality ([34, Proposition 2.2])

$$(\nu \bar{u} - S^*(y_d - S(\bar{u} + f)), \bar{u} - v) + \varphi(\bar{u}) - \varphi(v) \geq 0, \quad \forall v \in U_{ad}. \quad (17)$$

Through a pointwise discussion of the box constraints and an analysis of a Lagrange multiplier belonging to the subdifferential of φ in \bar{u} , [31] showed that (17) can be equivalently formulated as the nonlinear equation $\mathcal{F}(\bar{u}) = 0$, with $\mathcal{F} : L^2(\mathcal{D}) \rightarrow L^2(\mathcal{D})$ defined as

$$\mathcal{F}(u) := u - \frac{1}{\nu} (\max(0, \mathcal{T}u - \beta) + \min(0, \mathcal{T}u + \beta) - \max(0, \mathcal{T}u - \beta - \nu b) - \min(0, \mathcal{T}u + \beta - \nu a)), \quad (18)$$

where $\mathcal{T} : L^2(\mathcal{D}) \ni u \rightarrow -S^*(Su) + S^*(y_d - Sf) \in L^2(\mathcal{D})$. Notice that \mathcal{F} is nonsmooth due to the presence of the Lipschitz functions $\max(\cdot)$ and $\min(\cdot)$. Nevertheless, \mathcal{F} can be shown to be semismooth [25], provided that \mathcal{T} is continuously Fréchet differentiable, and further Lipschitz continuous interpreted as map from $\mathcal{T} : L^2(\mathcal{D}) \rightarrow L^r(\mathcal{D})$, with $r > 2$ [25, 35]. These conditions are satisfied also in our settings since \mathcal{T} is affine and further the adjoint variable p_ω , solution of (8) with $z = y_d - S(u + f)$, lies in $L^2(\Omega, H_0^1(\mathcal{D}))$ so that $\mathcal{T}u = \mathbb{E}[p_\omega] \in H_0^1(\mathcal{D}) \subset L^r(\mathcal{D})$, where $r > 2$ follows from the Sobolev embeddings.

Hence, to solve (18) we use the semismooth Newton method whose iteration reads for $k = 1, 2, \dots$ until convergence,

$$u^{k+1} = u^k + du^k, \quad \text{with} \quad \mathcal{G}(u^k)du^k = -\mathcal{F}(u^k), \quad (19)$$

$\mathcal{G}(u) : L^2(\mathcal{D}) \rightarrow L^2(\mathcal{D})$ being the generalized derivative of \mathcal{F} . Using the linearity of \mathcal{T} and considering the supports of the weak derivatives of $\max(0, x)$ and $\min(0, x)$, we obtain that

$$\mathcal{G}(u)[v] = v + \frac{1}{\nu} \chi_{(I^+ \cup I^-)} S^* S v, \quad (20)$$

where χ is the characteristic function of the union of the disjoint sets

$$I^+ = \{x \in \mathcal{D} : 0 \leq \mathcal{T}u - \beta \leq \nu b\} \quad \text{and} \quad I^- = \{x \in \mathcal{D} : \nu a \leq \mathcal{T}u + \beta \leq 0\}.$$

It is possible to show that the generalized derivative $\mathcal{G}(u)$ is invertible with bounded inverse for all u , the proof being identical to the deterministic case treated in [36]. This further implies that the semismooth Newton method (19) converges locally superlinearly [35]. We briefly summarize these results in the following proposition.

Proposition 2 *Let the initialization u^0 be sufficiently close to the solution \bar{u} of (16). Then the iterates u^k generated by (19) converge superlinearly to $\bar{u} \in L^2(\mathcal{D})$.*

Introducing the supporting variables dy_ω^k and dp_w^k in $L^2(\Omega; H_0^1(\mathcal{D}))$, the semismooth Newton equation $\mathcal{G}(u^k)du^k = -\mathcal{F}(u^k)$ may be rewritten as the

Algorithm 2 Globalized semismooth Newton Algorithm to solve $\mathbf{F}(\mathbf{u}) = 0$

Require: \mathbf{u}^0 , $\text{Tol} \in \mathbb{R}^+$, $\sigma, \rho \in (0, 1)$.

- 1: $\mathbf{y}_j^0 = A_j^{-1}(M_s(\mathbf{f} + \mathbf{u}^0))$, $\mathbf{p}_j^0 = (A_j^\top)^{-1}(M_s(\mathbf{y}_d - \mathbf{y}_j^0))$, $j = 1, \dots, N$.
 - 2: Set $k = 0$ and define I_0^+ and I_0^- using (24).
 - 3: **while** $\phi(\mathbf{u}^k) > \text{Tol}$ **do**
 - 4: Solve (23) calling Alg. 1 until convergence.
 - 5: Set $\gamma = 1$
 - 6: **while** $\phi(\mathbf{u}^k + \gamma \mathbf{d}\mathbf{u}^k) - \phi(\mathbf{u}^k) > -\sigma\phi(\mathbf{u}^k)$ **do**
 - 7: $\gamma = \rho\gamma$.
 - 8: **end while**
 - 9: Update $\mathbf{u}^{k+1} = \mathbf{u}^k + \gamma \mathbf{d}\mathbf{u}^k$, $\mathbf{y}_j^{k+1} = \mathbf{y}_j^k + \gamma \mathbf{d}\mathbf{y}_j^k$, $\mathbf{p}_j^{k+1} = \mathbf{p}_j^k + \gamma \mathbf{d}\mathbf{p}_j^k$,
 $j = 1, \dots, N$.
 - 10: Update I_k^+ and I_k^- using (24).
 - 11: Set $k = k + 1$.
 - 12: **end while**
 - 13: **return** $\mathbf{u}^k, \mathbf{y}_j^k$ and \mathbf{p}_j^k , $j = 1, \dots, N$.
-

notation of (2), it holds

$$(G)_{i,i} + d_i^\top \text{diag}(a_i)^{-1} \text{diag}(c_i) \text{diag}(a_i)^{-1} e_i = (M_s)_{i,i} + (M_s)_{i,i}^3 \sum_{j=1}^N w_j (A_j)_{i,i}^{-2} > 0$$

if $i \in I^+ \cup I^-$, and

$$(G)_{i,i} + d_i^\top \text{diag}(a_i)^{-1} \text{diag}(c_i) \text{diag}(a_i)^{-1} e_i = (M_s)_{i,i} > 0,$$

if $i \notin I^+ \cup I^-$. The collective multigrid iteration is then well-defined.

The overall semismooth Newton Algorithm is summarized in Algorithm 2. At each iteration we solve (23) using the collective multigrid algorithm (line 4) and update the active sets given the new iteration (line 10). Notice that in order to globalize the convergence, we consider a line-search step (lines 6-8) performed on the merit function $\phi(\mathbf{u}) = \sqrt{\mathbf{F}(\mathbf{u})^\top M_s \mathbf{F}(\mathbf{u})}$ [37].

4.1 Numerical experiments

In this section we test the semismooth Newton algorithm for the solution of (18) and the collective multigrid algorithm to solve the related optimality system (23). We consider the random PDE-constraint (14) with the random diffusion coefficient (15). The semismooth iteration is stopped when $\phi(\mathbf{u}^k) < 10^{-9}$. The inner linear solvers are stopped when the relative (unpreconditioned) residual is smaller than 10^{-11} .

Table 3 reports the number of semismooth Newton iterations and in brackets the averaged number of iterations of the V-cycle algorithm used as a solver (left) or as preconditioner for GMRES (right). Table 3 confirms the

effectiveness of the multigrid algorithm, which requires essentially the same computational effort than in the linear-quadratic case.

Table 3 Number of semismooth Newton iterations, and average number of V-cycle iterations and preconditioned GMRES iterations (in brackets).

| σ^2 | 0.1 | 0.5 | 1 | 1.5 |
|------------|------------------|-----------------|----------------|-----------------|
| It. | 3 (22.33 - 10.3) | 4 (22.5 - 10.5) | 7(22.8 - 11.7) | 8 (23.1 - 11.7) |

$N_h = 961, \nu = 10^{-4}, \beta = 10^{-2}, N = 125, N_L = 3, L^2 = 0.5, b = 50, a = -50.$

| $N_h(N_L)$ | 225 (2) | 961 (3) | 3969 (4) |
|------------|-------------------|-----------------|------------------|
| It. | 4 (21.75 - 11.25) | 4 (22.5 - 10.5) | 4 (22.5 - 10.25) |

$\nu = 10^{-4}, \beta = 10^{-2}, N = 125, \sigma^2 = 0.5, L^2 = 0.5, b = 50, a = -50.$

| N | 8 | 27 | 64 | 125 |
|-----|--------------|-----------------|----------------|-----------------|
| It. | 4 (21 - 9.7) | 4 (21.5 - 10.5) | 5 (22.2 - 9.6) | 4 (22.5 - 10.5) |

$N_h = 961, \nu = 10^{-4}, \beta = 10^{-2}, \sigma^2 = 0.5, L^2 = 0.5, b = 50, a = -50.$

| β | 0 | 10^{-4} | 10^{-3} | 10^{-2} |
|---------|-----------------|-------------|-------------|-----------------|
| It. | 5 (22.2 - 10.2) | 4 (22 - 11) | 5 (22 - 11) | 4 (22.5 - 10.5) |

$N_h = 961, \nu = 10^{-4}, N = 125, \sigma^2 = 0.5, L^2 = 0.5, b = 50, a = -50.$

More challenging is the limit $\nu \rightarrow 0$ reported in Table 4. The performance of both the (globalized) semismooth Newton iteration and the inner multigrid solver deteriorates. The convergence of the outer nonlinear algorithm can be improved by performing a continuation method, namely we consider a sequence of $\nu = 10^{-j}, j = 2, \dots, 8$, and we start the j -th problem using as initial condition the optimal solution computed for $\nu = 10^{-j+1}$. Concerning the inner solver, the stand-alone multigrid algorithm struggles since for small values of ν the optimal control is of bang-bang type, that is satisfies $u = a, u = b$ or $u = 0$ for almost every point of the mesh (for $\nu = 10^{-8}$ only seven nodes are nonactive at the optimum). The matrices H^k are then close to zero, and the multigrid hierarchy struggles to capture changes at such small scale. Nevertheless, the multigrid algorithm remains a very efficient preconditioner for GMRES even in this challenging limit.

Fig. 1 shows a sequence of optimal controls for different values of β with and without box-constraints. The optimal control for $\beta = 0$ and without box-constraints corresponds to the minimizer of the linear-quadratic OCP (5). We observe that L^1 penalization indeed induces sparsity, since the optimal controls are more and more localized as β increases. Numerically we have

Table 4 Number of semismooth Newton iterations, and of V-cycle iterations and preconditioned GMRES iterations (in brackets). In the second row, the semismooth Newton method starts from a warm-up initial guess obtained through continuation.

| ν | 10^{-2} | 10^{-4} | 10^{-6} | 10^{-8} |
|-------|--------------|-----------------|------------------|-------------------|
| It. | 2 (22 - 9.5) | 4 (22.5 - 10.5) | 23 (27.5 - 12.3) | 52 (45.1 - 13.7) |
| It. | 2 (22 - 9.5) | 4 (22 - 10.5) | 5 (27.6 - 11.8) | 14 (68.07 - 17.2) |

$N_h = 961, N = 125, N_L = 3, \sigma^2 = 0.5, L^2 = 0.5, b = 50, a = -50.$

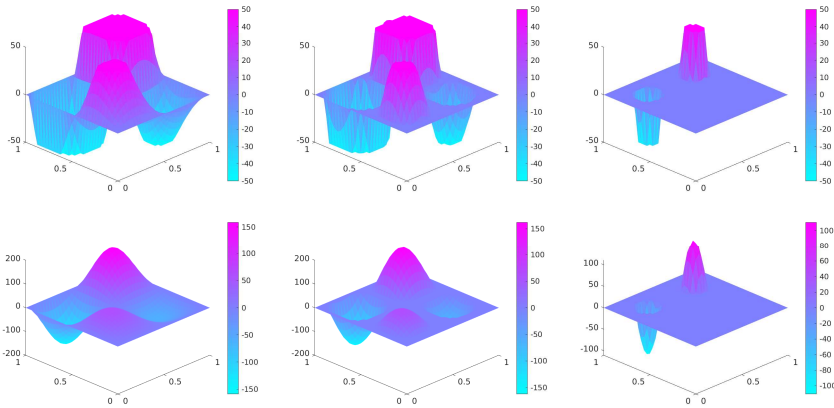


Fig. 1 From left to right: optimal control computed for $\beta \in \{0, 5 \cdot 10^{-3}, 5 \cdot 10^{-2}\}$ with (top row) and without (bottom row) box constraints: $a = -50$, $b = 50$.

verified that for sufficiently large β , the optimal control is identically equal to zero, a property shown in [31].

5 A risk-averse optimal control problem under uncertainty

In this section we consider an instance of risk-averse OCPUU. This class of problems has recently drawn lot of attention since in engineering applications it is important to compute a control that minimizes the quantity of interest even in rare, but often troublesome, scenarios [2, 6, 38]. As a risk-measure [39], we use the Conditional Value-At-Risk (CVaR) of confidence level λ , $\lambda \in (0, 1)$,

$$\text{CVaR}_\lambda(X) := \mathbb{E}[X | X \geq \text{VaR}_\lambda(X)], \quad \forall X \in L^1(\Omega; \mathbb{R}),$$

that is, the expected value of a quantity of interest X given that the latter is greater than or equal to its λ -quantile, here denoted by $\text{VaR}_\lambda(X)$. Rockafellar and Uryasev [40] proved that $\text{CVaR}_\lambda(X)$ admits the equivalent formulation

$$\text{CVaR}_\lambda(X) = \inf_{t \in \mathbb{R}} \left\{ t + \frac{1}{1-\lambda} \mathbb{E}[(X-t)^+] \right\}, \quad (25)$$

where $(\cdot)^+ := \max(0, \cdot)$, if the distribution of X does not have an atom at $\text{VaR}_\lambda(X)$. In order to use tools from smooth optimization, we rely on a smoothing approach proposed in [2], which consists in replacing $(\cdot)^+$ with a smooth function g_ε , $\varepsilon \in \mathbb{R}^+$, such that $g_\varepsilon \rightarrow (\cdot)^+$ in some functional norm as

16 *A MG solver for PDE-constrained optimization with uncertain inputs*

$\varepsilon \rightarrow 0$. Specifically, we choose the C^2 -differentiable approximation

$$g_\varepsilon(x) = \begin{cases} 0 & \text{if } x \leq -\frac{\varepsilon}{2}, \\ \frac{(x-\frac{3}{2})^3}{\varepsilon^2} - \frac{(x-\frac{\varepsilon}{2})^4}{2\varepsilon^3} & \text{if } x \in (-\frac{\varepsilon}{2}, \frac{\varepsilon}{2}), \\ x & \text{if } x \geq \frac{\varepsilon}{2}. \end{cases} \quad (26)$$

Then, the smoothed risk-averse OCPUU is

$$\begin{aligned} \min_{u \in L^2(\mathcal{D}), t \in \mathbb{R}} \quad & t + \frac{1}{1-\lambda} \mathbb{E} \left[g_\varepsilon \left(\frac{1}{2} \|y_\omega - y_d\|_{L^2(\mathcal{D})}^2 - t \right) \right] + \frac{\nu}{2} \|u\|_{L^2(\mathcal{D})}^2, \\ \text{subject to} \quad & \\ a_\omega(y_\omega, v) = (u + f, v) \quad & \forall v \in V, \mathbb{P}\text{-a.e. } \omega \in \Omega. \end{aligned} \quad (27)$$

where $\nu \in \mathbb{R}^+$ and $\lambda \in [0, 1)$. The well-posedness of (27), the differentiability of its objective functional, as well as bounds for the error introduced by replacing $(\cdot)^+$ with $g_\varepsilon(\cdot)$, have been analyzed in [2]. Further, defining $Q_\omega = \frac{1}{2} \|y_\omega - y_d\|_{L^2(\mathcal{D})}^2 - t$, the optimality conditions form the nonlinear system,

$$\begin{aligned} a_\omega(v, p_\omega) - \frac{g'_\varepsilon(Q_\omega)}{1-\lambda} (y_d - y_\omega, v) &= 0, & \forall v \in V, \mathbb{P}\text{-a.e. } \omega \in \Omega, \\ (\nu u - \mathbb{E}[p_\omega], v) &= 0, & \forall v \in L^2(\mathcal{D}) \\ a_\omega(y_\omega, v) - (u + f, v) &= 0, & \forall v \in V, \mathbb{P}\text{-a.e. } \omega \in \Omega, \\ 1 - \frac{1}{1-\lambda} \mathbb{E}[g'_\varepsilon(Q_\omega)] &= 0, \end{aligned} \quad (28)$$

Approximating V and \mathbb{E} with V_h and $\widehat{\mathbb{E}}$, and letting $\tilde{\mathbf{x}} = (\mathbf{y}, \mathbf{u}, \mathbf{p}, t)$, the finite-dimensional discretization of (28) corresponds to the nonlinear system $\tilde{\mathbf{F}}(\tilde{\mathbf{x}}) = \mathbf{0}$, where $\tilde{\mathbf{F}} : \mathbb{R}^{(2N+1)N_h+1} \rightarrow \mathbb{R}^{(2N+1)N_h+1}$,

$$\tilde{\mathbf{F}}(\tilde{\mathbf{x}}) = \begin{pmatrix} \tilde{\mathbf{F}}_1(\tilde{\mathbf{x}}) \\ \tilde{\mathbf{F}}_2(\tilde{\mathbf{x}}) \\ \tilde{\mathbf{F}}_3(\tilde{\mathbf{x}}) \\ \tilde{\mathbf{F}}_4(\tilde{\mathbf{x}}) \end{pmatrix} = \begin{pmatrix} \tilde{M}(\mathbf{y} - I\mathbf{y}_d) + A^\top \mathbf{p} \\ \nu M_s \mathbf{u} - M_s \widehat{\mathbb{E}}[\mathbf{p}] \\ A\mathbf{y} - M_s(I\mathbf{u} + \mathbf{f}) \\ 1 - \frac{1}{1-\lambda} \widehat{\mathbb{E}}[g'_\varepsilon(Q_\omega)] \end{pmatrix}, \quad (29)$$

with $A = \text{diag}(A_1, \dots, A_N)$, $I = [I_{N_h}, \dots, I_{N_h}] \in \mathbb{R}^{N_h \times N_h N}$, I_h being the identity matrix, \mathbf{y}_d is the discretization of y_d , and

$$\tilde{M} = \text{diag} \left(\frac{g'_\varepsilon(Q_{\omega_1})}{1-\lambda} M_s, \dots, \frac{g'_\varepsilon(Q_{\omega_N})}{1-\lambda} M_s \right), \text{ with } Q_{\omega_j} := \frac{1}{2} (\mathbf{y}_j - \mathbf{y}_d)^\top M_s (\mathbf{y}_j - \mathbf{y}_d) - t,$$

for $j = 1, \dots, N$.

A possible approach to solve (29) is to use a Newton method, which given $\mathbf{x}^k = (\mathbf{y}^k, \mathbf{u}^k, \mathbf{p}^k, t^k)$ computes the corrections $\widetilde{\mathbf{d}\mathbf{x}}^k = (\mathbf{d}\mathbf{y}^k, \mathbf{d}\mathbf{u}^k, \mathbf{d}\mathbf{p}^k, dt^k)$

solution of $\tilde{\mathbf{J}}^k \tilde{\mathbf{d}}^k = -\tilde{\mathbf{F}}(\tilde{\mathbf{x}}^k)$, where

$$\tilde{\mathbf{J}}^k := \begin{pmatrix} C_1(\mathbf{y}_1^k, t^k) & & & A_1^\top & & & -\mathbf{v}_1^k \\ & \ddots & & & & \ddots & \vdots \\ & & C_N(\mathbf{y}_N^k, t^k) & & & & -\mathbf{v}_N^k \\ & & & \nu M_s & -w_1 M_s & \dots & -w_N M_s \\ & A_1 & & -M_s & & & \\ & & \ddots & \vdots & & & \\ & & & A_N & -M_s & & \\ -w_1 (\mathbf{v}_1^k)^\top & \dots & -w_N (\mathbf{v}_N^k)^\top & & & & \frac{\widehat{\mathbb{E}}[g_\varepsilon''(Q_\omega^k)]}{1-\lambda} \end{pmatrix}, \quad (30)$$

with

$$Q_{\omega_i}^k := \frac{1}{2}(\mathbf{y}_i^k - \mathbf{y}_d)^\top M_s(\mathbf{y}_i^k - \mathbf{y}_d) - t^k, \quad (31)$$

$$C_i(\mathbf{y}_i^k, t^k) := \frac{1}{1-\lambda} (g'_\varepsilon(Q_{\omega_i}^k)M_s + g''_\varepsilon(Q_{\omega_i}^k)M_s(\mathbf{y}_i^k - \mathbf{y}_d)(\mathbf{y}_i^k - \mathbf{y}_d)^\top M_s), \quad (32)$$

$$\mathbf{v}_i^k := \frac{1}{1-\lambda} g''_\varepsilon(Q_{\omega_i}^k)M_s(\mathbf{y}_i^k - \mathbf{y}_d), \quad (33)$$

for $i = 1, \dots, N$. Unfortunately, $\tilde{\mathbf{J}}^k$ can be singular away from the optimum, in particular whenever $\widehat{\mathbb{E}}[g''_\varepsilon(Q_\omega^k)] = 0$ which implies

$$g''_\varepsilon\left(\frac{1}{2}(\mathbf{y}_j^k - \mathbf{y}_d)^\top M_s(\mathbf{y}_j^k - \mathbf{y}_d) - t^k\right) = 0, \quad \forall j = 1, \dots, N, \quad (34)$$

which is not unlikely for small ε since $\text{supp}(g''_\varepsilon) = (-\frac{\varepsilon}{2}, \frac{\varepsilon}{2})$. Splitting strategies have been proposed (e.g. [41] in a reduced approach), in which whenever (34) is satisfied, an intermediate value of t is computed by solving $\tilde{F}_4(t; \mathbf{y}, \mathbf{u}, \mathbf{p}) = 0$ so to violate (34). In the next section, we discuss a similar splitting approach. To speed up the convergence of the outer nonlinear algorithm, we use a preconditioned Newton method based on nonlinear elimination [42]. At each iteration we will need to invert saddle-point matrices like (2), possibly several times. To do so, we rely on the collective multigrid algorithm.

5.1 Nonlinear preconditioned Newton method

Nonlinear elimination is a nonlinear preconditioning technique based on the identification of variables and equations of \mathbf{F} (e.g. strong nonlinearities) that slow down the convergence of Newton method. These components are then eliminated through the solution of a local nonlinear problem at every step of an outer Newton. This elimination step provides a better initial guess for the outer iteration, so that a faster convergence is achieved [42, 43].

In light of the possible singularity of $\tilde{\mathbf{J}}$, we split the discretized variables $\tilde{\mathbf{x}}$ into $\tilde{\mathbf{x}} = (\mathbf{x}, t)$, and we aim to eliminate the variables \mathbf{x} to obtain a scalar nonlinear equation only for t . To do so, we partition (28) as

$$\tilde{\mathbf{F}} \begin{pmatrix} \mathbf{x} \\ t \end{pmatrix} = \begin{pmatrix} \mathbf{F}_1(\mathbf{x}, t) \\ F_2(\mathbf{x}, t) \end{pmatrix} = \begin{pmatrix} \mathbf{0} \\ 0 \end{pmatrix}, \quad (35)$$

where $\mathbf{F}_1 = (\tilde{\mathbf{F}}_1(\mathbf{x}, t), \tilde{\mathbf{F}}_2(\mathbf{x}, t), \tilde{\mathbf{F}}_3(\mathbf{x}, t))$ and $F_2(\mathbf{x}, t) = \tilde{F}_4(\mathbf{x}, t)$. Similarly, $\tilde{\mathbf{J}}$ is partitioned into

$$\tilde{\mathbf{J}} = \begin{pmatrix} \mathbf{J}_{1,1} & \mathbf{J}_{1,2} \\ \mathbf{J}_{2,1} & J_{2,2} \end{pmatrix}$$

whose blocks have dimensions $\mathbf{J}_{1,1} \in \mathbb{R}^{(2N+1)N_h \times (2N+1)N_h}$, $\mathbf{J}_{1,2} \in \mathbb{R}^{(2N+1)N_h \times 1}$, $\mathbf{J}_{2,1} \in \mathbb{R}^{1 \times (2N+1)N_h}$, and $\mathbf{J}_{2,2} \in \mathbb{R}$. Notice that $\mathbf{J}_{1,1}$ is always nonsingular, while $\mathbf{J}_{2,1}$, $\mathbf{J}_{1,2}$ and $J_{2,2}$ are identically zero if (34) is verified. Thus \mathbf{F}_1 allows us to define an implicit map $h : \mathbb{R} \rightarrow \mathbb{R}^{(2N+1)N_h}$, such that $\mathbf{F}_1(h(t), t) = 0$, so that the first set of nonlinear equations in (35) are satisfied. We are then left to solve the nonlinear scalar equation

$$F(t) = 0, \quad \text{where} \quad F(t) := F_2(h(t), t). \quad (36)$$

To do so using the Newton method, we need the derivative of $F(t)$ evaluated at $t = t^k$ which, using implicit differentiation, can be computed as

$$F'(t^k) = J_{2,2}(h(t^k), t^k) - \mathbf{J}_{2,1}(h(t^k), t^k) (\mathbf{J}_{1,1}(h(t^k), t^k))^{-1} \mathbf{J}_{1,2}(h(t^k), t^k).$$

The nonlinear preconditioned Newton method is described in Alg. 3, and consists in solving (36) with Newton method. However, to overcome the possible singularity of $J_{2,2}^k$, $\mathbf{J}_{1,2}^k$ and $\mathbf{J}_{2,1}^k$, we check at each iteration k if (34) is satisfied, and in the affirmative case we update \mathbf{x}^k by solving $\mathbf{F}_1(\mathbf{x}^{k+1}, t^k) = 0$ using Newton method, and update t^k by solving $F_2(\mathbf{x}^k, t^{k+1}) = 0$. Notice further, that each iteration of the backtracking line-search requires to solve $F_1(h(t), t) = 0$ using Newton method, thus additional linear systems with matrix $\mathbf{J}_{1,1}$ must be solved.

We report that we also tried to eliminate t by computing the map l such that $F_2(\mathbf{x}, l(\mathbf{x})) = 0$, while iterating on the variable \mathbf{x} . This has the advantage that l can be evaluated very cheaply, being a scalar equation. However, we needed many more iterations both of the outer Newton method, and consequently of the inner linear solver. Thus, according to our experience, this second approach was less efficient and appealing.

5.2 Numerical experiments

In this section we report numerical tests to assess the performance of the preconditioned Newton algorithm to solve (29), and of the collective multigrid algorithm to invert the matrix $\mathbf{J}_{1,1}$. We consider the random PDE-constraint

Algorithm 3 Nonlinear preconditioned Newton method to solve $\widetilde{\mathbf{F}}(\widetilde{\mathbf{x}}) = 0$.

Require: $t^0, \text{Tol} \in \mathbb{R}^+, \sigma, \rho \in (0, 1)$.

- 1: Compute $\mathbf{x}^0 = h(t^0)$ solving $\mathbf{F}_1(\mathbf{x}^0; t^0) = 0$ using the Newton method.
 - 2: Set $k = 0$.
 - 3: **while** $|F(t^k)| > \text{Tol}$ **do**
 - 4: **if** (34) is satisfied **then**
 - 5: Compute \mathbf{x}^{k+1} and t^{k+1} solving $\mathbf{F}(\mathbf{x}^{k+1}; t^k) = 0$ and $\widetilde{F}_4(\mathbf{x}^k; t^{k+1}) = 0$.
 - 6: **else**
 - 7: Compute Newton's direction $d = -(F'(t^k))^{-1}F(t^k)$.
 - 8: Set $\gamma = 1$ and compute $\mathbf{x} = h(t^k + \gamma d)$ solving $\mathbf{F}_1(\mathbf{x}; t^k + d) = 0$.
 - 9: **while** $|F(t^k + \gamma d)| - |F(t^k)| > -\sigma|F(t^k)|$ **do**
 - 10: Set $\gamma = \rho\gamma$.
 - 11: Compute $\mathbf{x} = h(t^k + \gamma d)$ solving $\mathbf{F}_1(\mathbf{x}; t^k + \gamma d) = 0$.
 - 12: **end while**
 - 13: Set $t^{k+1} = t^k + \gamma d, \mathbf{x}^{k+1} = \mathbf{x}, k = k + 1$.
 - 14: **end if**
 - 15: **end while**
 - 16: **return** t^{k+1} and \mathbf{x}^{k+1} .
-

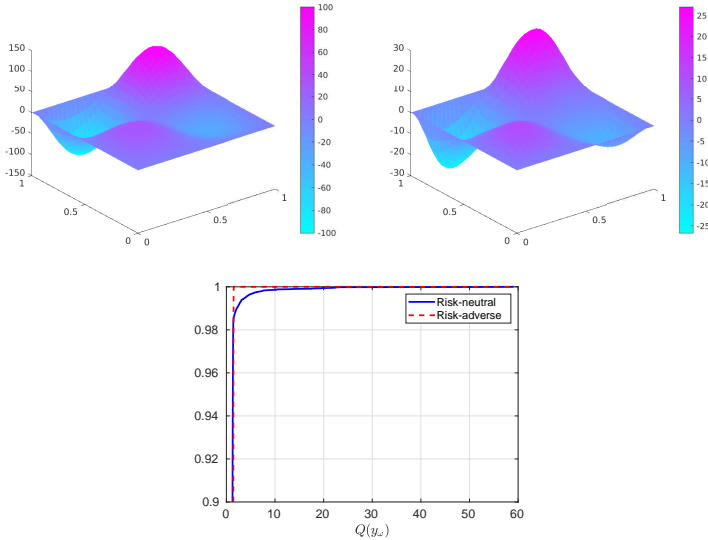
(14) with the random diffusion coefficient (15). Table 5 reports the number of outer and inner Newton iterations, and the average number of V-cycle iterations and of preconditioned GMRES iterations to solve the linear systems at each (inner/outer) Newton iterations. The outer Newton iteration is stopped when $|F(t^k)| \leq 10^{-6}$, the inner Newton method to compute $h(\cdot)$ is stopped when $\|\mathbf{F}_{1,1}(\mathbf{x}; t^k)\|_2 \leq 10^{-9}$, and the linear solvers are stopped when the (unpreconditioned) residual is smaller than 10^{-10} .

In Table 5, the number of outer Newton iterations is quite stable, while the number of inner Newton iterations varies between five and twenty iterations per outer iteration, essentially due to how difficult it is to compute the nonlinear map $h(t)$ by solving $\mathbf{F}_1(\mathbf{x}; t^k) = 0$ in line (5), (8) and (11) of Alg. 3. The average number of inner linear solvers iterations is quite stable as well. We emphasize that the top left blocks of $\mathbf{J}_{1,1}$ involve the matrices $C_i(\mathbf{y}_i^k, t^k)$ (see (32)) which contain a dense low-rank term if $g''_\varepsilon(Q_{\omega_i}^k) \neq 0$. Further, as $\varepsilon \rightarrow 0$, $g''_\varepsilon(\cdot)$ tends to a Dirac delta, so the dense term become dominant. Multigrid methods based on a pointwise relaxations are expected to be not very efficient for these matrices which may not be diagonally dominant. The standard V-cycle algorithm indeed struggles, however the Krylov acceleration performs much better as it handles these low-rank perturbation with smaller effort. We sometimes noticed that the GMRES residual stagnates after 20/30 iterations around $10^{-8}/10^{-9}$, due to a loss of orthogonality in the Krylov subspace. We allowed a maximum number of 80 GMRES iterations per linear system.

Figure 2 compares the two optimal controls obtained minimizing either $\mathbb{E}[Q(y_\omega)]$ or $\text{CVaR}_\lambda(Q(y_\omega))$, and cumulative distribution functions of $Q(y_{\omega_j})$

Table 5 Number of preconditioned Newton iterations, and of V-cycle iterations and preconditioned GMRES iterations (in brackets).

| $N_h(N_L)$ | 81 (2) | 361 (3) | 1521 (4) | |
|---|------------------------|-------------------------|--------------------------|-------------------------|
| It. | 6 - 61 - (33.4 - 18.2) | 7 - 74 - (34.2 - 17.2) | 7 - 79 - (30.1 - 26.7) | |
| $\nu = 10^{-4}$, $\lambda = 0.95$, $\varepsilon = 10^{-2}$, $N = 125$, $\sigma^2 = 1$, $L^2 = 0.5$. | | | | |
| N | 8 | 27 | 64 | 125 |
| It. | 4 - 20 - (19.3 - 13.2) | 8 - 188 - (32.3 - 17.3) | 5 - 50 - (27.8 - 15.7) | 7 - 85 - (22.9 - 14.9) |
| $N_h = 961$, $\nu = 10^{-4}$, $\lambda = 0.95$, $\varepsilon = 10^{-2}$, $\sigma^2 = 1$, $L^2 = 0.5$. | | | | |
| λ | 0 | 0.5 | 0.95 | 0.99 |
| It. | 0 - 1 - (21 - 15) | 6 - 80 - (20.4 - 14.2) | 6 - 85 - (22.9 - 14.9) | 7 - 124 - (34.9 - 17.3) |
| $N_h = 961$, $\nu = 10^{-4}$, $\varepsilon = 10^{-2}$, $N = 125$, $\sigma^2 = 1$, $L^2 = 0.5$. | | | | |
| ε | 10^{-1} | 10^{-2} | 10^{-3} | 10^{-4} |
| It. | 4 - 25 - (21.1 - 14.8) | 2 - 13 - (20.9 - 14.5) | 4 - 100 - (27.8 - 15.98) | 1 - 27 - (62.9 - 16.1) |
| $N_h = 961$, $\nu = 10^{-4}$, $\beta = 0.95$, $N = 125$, $\sigma^2 = 1$, $L^2 = 0.5$. | | | | |

**Fig. 2** Solution of the linear-quadratic OCP (top-left), solution of the smoothed risk-averse OCP with $\lambda = 0.99$ (top-right), and cumulative distribution function of the quantity of interest for the two controls.

for the two controls computed out-of-sample. The risk-averse control indeed minimizes the *risk* of having large values of $Q(y_\omega)$. The CVaR of level $\lambda = 0.99$ is respectively $\text{CVaR}_{0.99}(Q(y_\omega)) = 6.7028$ for the risk-neutral control and $\text{CVaR}_{0.99}(Q(y_\omega)) = 1.4760$ for the risk-averse control.

6 Conclusion

We have presented a multigrid method to solve the large saddle point linear systems that typically arise in full-space approaches to solve OCPUU. We tested the algorithm as a iterative solver and as a preconditioner on three test cases: a linear-quadratic OCPUU, a nonsmooth OCPUU, and a risk-averse nonlinear OCPUU. Overall, the multigrid method shows very good performances and robustness with respect to the several parameters of the problems considered.

7 Declarations

Ethical Approval: Not applicable.

Data Availability: The codes used in this study are available from the corresponding author on reasonable request.

Competing interests: The authors declare that they have no conflict of interest.

Funding: Not applicable.

Authors' contributions: All authors contributed equally to the manuscript.

Acknowledgements: Gabriele Ciaramella and Tommaso Vanzan are members of GNCS (Gruppo Nazionale per il Calcolo Scientifico) of INdAM. The present research is part of the activities of “Dipartimento di Eccellenza 2023-2027”.

References

- [1] Kouri, D.P., Shapiro, A.: Optimization of PDEs with uncertain inputs. In: *Frontiers in PDE-Constrained Optimization*, pp. 41–81. Springer, New York (2018)
- [2] Kouri, D.P., Surowiec, T.M.: Risk-averse PDE-constrained optimization using the conditional value-at-risk. *SIAM Journal on Optimization* **26**(1), 365–396 (2016)
- [3] Martínez-Frutos, J., Esparza, F.: *Optimal Control of PDEs Under Uncertainty: an Introduction with Application to Optimal Shape Design of Structures*. Springer, Heidelberg (2018)
- [4] Guth, P.A., Kaarnioja, V., Kuo, F., Schillings, C., Sloan, I.H.: A Quasi-Monte Carlo method for optimal control under uncertainty. *SIAM/ASA Journal on Uncertainty Quantification* **9**(2), 354–383 (2021)
- [5] Geiersbach, C., Wollner, W.: A stochastic gradient method with mesh refinement for PDE-constrained optimization under uncertainty. *SIAM Journal on Scientific Computing* **42**(5), 2750–2772 (2020)

- [6] Antil, H., Dolgov, S., Onwunta, A.: TTRISK: Tensor train decomposition algorithm for risk averse optimization. arXiv preprint arXiv:2111.05180 (2021)
- [7] Nobile, F., Vanzan, T.: A combination technique for optimal control problems constrained by random PDEs. arXiv preprint arXiv:2211.00499 (2022)
- [8] Eigel, M., Neumann, J., Schneider, R., Wolf, S.: Risk averse stochastic structural topology optimization. *Computer Methods in Applied Mechanics and Engineering* **334**, 470–482 (2018)
- [9] Asadpoure, A., Tootkaboni, M., Guest, J.K.: Robust topology optimization of structures with uncertainties in stiffness - application to truss structures. *Computers & Structures* **89**(11), 1131–1141 (2011). *Computational Fluid and Solid Mechanics* 2011
- [10] Kouri, D.P., Heinkenschloss, M., Ridzal, D., van Bloemen Waanders, B.G.: A trust-region algorithm with adaptive stochastic collocation for PDE optimization under uncertainty. *SIAM Journal on Scientific Computing* **35**(4), 1847–1879 (2013)
- [11] Kouri, D.P., Ridzal, D.: Inexact Trust-Region methods for PDE-constrained optimization, pp. 83–121. Springer, New York, NY (2018)
- [12] Nobile, F., Vanzan, T.: Preconditioners for robust optimal control problems under uncertainty. *Numerical Linear Algebra with Applications* **30**(2), 2472 (2023)
- [13] Borzi, A., Kunisch, K.: A multigrid scheme for elliptic constrained optimal control problems. *Computational Optimization and Applications* **31**(3), 309–333 (2005)
- [14] Borzi, A., Schulz, V.: Multigrid methods for PDE optimization. *SIAM review* **51**(2), 361–395 (2009)
- [15] Takacs, S., Zulehner, W.: Convergence analysis of multigrid methods with collective point smoothers for optimal control problems. *Computing and Visualization in Science* **14**(3), 131–141 (2011)
- [16] Borzi, A., von Winckel, G.: Multigrid methods and sparse-grid collocation techniques for parabolic optimal control problems with random coefficients. *SIAM Journal on Scientific Computing* **31**(3), 2172–2192 (2009)
- [17] Borzi, A.: Multigrid and sparse-grid schemes for elliptic control problems with random coefficients. *Computing and visualization in science* **13**(4),

153–160 (2010)

- [18] Rosseel, E., Wells, G.N.: Optimal control with stochastic PDE constraints and uncertain controls. *Computer Methods in Applied Mechanics and Engineering* **213**, 152–167 (2012)
- [19] Kouri, D.P.: A multilevel stochastic collocation algorithm for optimization of pdes with uncertain coefficients. *SIAM/ASA Journal on Uncertainty Quantification* **2**(1), 55–81 (2014)
- [20] Lord, G.J., Powell, C.E., Shardlow, T.: *An Introduction to Computational Stochastic PDEs*. Cambridge Texts in Applied Mathematics. Cambridge University Press, Cambridge (2014)
- [21] Charrier, J., Scheichl, R., Teckentrup, A.L.: Finite element error analysis of elliptic PDEs with random coefficients and its application to multilevel Monte Carlo methods. *SIAM Journal on Numerical Analysis* **51**(1), 322–352 (2013)
- [22] Cohn, D.L.: *Measure Theory: Second Edition*. Birkhäuser, New York (2013)
- [23] Tröltzsch, F.: *Optimal Control of Partial Differential Equations: Theory, Methods, and Applications*. Graduate studies in mathematics. American Mathematical Society, New York (2010)
- [24] Lions, J.L.: *Optimal Control of Systems Governed by Partial Differential Equations*. Die Grundlehren der mathematischen Wissenschaften in Einzeldarstellungen. Springer, Heidelberg (1971)
- [25] Hinze, M., Pinnau, R., Ulbrich, M., Ulbrich, S.: *Optimization with PDE Constraints vol. 23*. Springer, Heidelberg (2008)
- [26] Charrier, J.: Strong and weak error estimates for elliptic partial differential equations with random coefficients. *SIAM Journal on Numerical Analysis* **50**(1), 216–246 (2012)
- [27] Babuška, I., Nobile, F., Tempone, R.: A stochastic collocation method for elliptic partial differential equations with random input data. *SIAM review* **52**(2), 317–355 (2010)
- [28] Rees, T., Dollar, H.S., Wathen, A.: Optimal solvers for PDE-constrained optimization. *SIAM Journal on Scientific Computing* **32**(1), 271–298 (2010)
- [29] Pearson, J.W., Wathen, A.: A new approximation of the Schur complement in preconditioners for PDE-constrained optimization. *Numerical*

- 24 *A MG solver for PDE-constrained optimization with uncertain inputs*
 Linear Algebra with Applications **19**(5), 816–829 (2012)
- [30] Ciaramella, G., Gander, M.J.: Iterative Methods and Preconditioners for Systems of Linear Equations. SIAM, Philadelphia, PA (2022)
- [31] Stadler, G.: Elliptic optimal control problems with l^1 -control cost and applications for the placement of control devices. Computational Optimization and Applications **44**(2), 159–181 (2009)
- [32] Casas, E.: A review on sparse solutions in optimal control of partial differential equations. SeMA Journal **74**(3), 319–344 (2017)
- [33] Li, C., Stadler, G.: Sparse solutions in optimal control of PDEs with uncertain parameters: The linear case. SIAM Journal on Control and Optimization **57**(1), 633–658 (2019)
- [34] Ekeland, I., Temam, R.: Convex Analysis and Variational Problems. SIAM, Philadelphia, PA (1999)
- [35] Ulbrich, M.: Semismooth Newton Methods for Variational Inequalities and Constrained Optimization Problems in Function Spaces. SIAM, Philadelphia, PA (2011)
- [36] Stadler, G.: Errata: Elliptic optimal control problems with L^1 -control cost and applications for the placement of control devices (2008)
- [37] Martínez, J., Qi, L.: Inexact newton methods for solving nonsmooth equations. Journal of Computational and Applied Mathematics **60**(1-2), 127–145 (1995)
- [38] Kouri, D.P., Surowiec, T.M.: Existence and optimality conditions for risk-averse PDE-constrained optimization. SIAM/ASA Journal on Uncertainty Quantification **6**(2), 787–815 (2018)
- [39] Shapiro, A., Dentcheva, D., Ruszczyński, A.: Lectures on Stochastic Programming: Modeling and Theory, Second Edition. SIAM, Philadelphia, PA (2014)
- [40] Rockafellar, R.T., Uryasev, S., *et al.*: Optimization of conditional value-at-risk. Journal of risk **2**, 21–42 (2000)
- [41] Markowski, M.: Efficient solution of smoothed risk-adverse PDE-constrained optimization problems. PhD thesis, Rice University (2022)
- [42] Lanzkron, P.J., Rose, D.J., Wilkes, J.T.: An analysis of approximate non-linear elimination. SIAM Journal on Scientific Computing **17**(2), 538–559 (1996)

- [43] Yang, H., Hwang, F.-N., Cai, X.-C.: Nonlinear preconditioning techniques for full-space lagrange–newton solution of PDE-constrained optimization problems. *SIAM Journal on Scientific Computing* **38**(5), 2756–2778 (2016)